Creating multimode squeezed states and Greenberger-Horne-Zeilinger entangled states using atomic coherent effects

Xiao Liang, Xiangming Hu, and Chang He

Phys. Rev. A **85**, 032329 — Published 26 March 2012

DOI: 10.1103/PhysRevA.85.032329

Creating multimode squeezes states and Greenberger-Horne-Zeilinger entangled states using atomic coherent effects

Xiao Liang, Xiangming Hu* and Chang He
College of Physical Science and Technology, Central China Normal University, Wuhan 430079, People's Republic of China

We propose a scalable scheme for a unitary multimode operator using an optical cavity with an atomic ensemble. We exemplify three-mode and four-mode cases and engineer the squeeze operators that are decoupled from the atomic degrees of freedom. The squeeze parameter can be large since they are proportional to the number of atoms. Using the input-output theory we show that ideal squeezed states and perfect squeezing could be approached at the output. At the same time, we show that it is possible to obtain tripartite and quadripartite Greenberger-Horne-Zeilinger entangled states for continuous variables. The responsible mechanism for both the multimode squeezing and the genuine multipartite entanglement is based on the atomic coherence controlled parametric interactions. The scalability of the scheme is simply obtained by including more transitions in the atomic system.

PACS numbers: 03.67.Bg, 42.50.Pq, 42.50.Dv, 32.80.Qk

I. INTRODUCTION

The reduction of quantum noise is one of the important issues in quantum optics, laser physics and nonlinear optics since Caves *et al.* [1] first noted the possibilities of manipulating quantum fluctuations with the aim of precision measurement. Squeezing is defined, for an optical field, when the fluctuations in a certain quadrature are reduced below the vacuum level at the expense of increasing them in its canonically conjugate variable [2, 3]. Since then great effort has been paid to it. Either the theoretical proposals have been presented or the experimental implementations have been performed. Squeezing can happen either for a single-mode quadrature or for a two-mode quadrature [2, 3]. Of extreme importance is the close correlation of the two-mode squeezing to the continuous variable (CV) entanglement [4, 5], which is the important resources for the quantum information and quantum computation [6–8]. For example, by using the entangled squeezed states of the electromagnetic field one realized the CV teleportation [9–11]. The two-mode (polarization) squeezing was realized by employing Kerr nonlinearity in optical fibers and with cold atomic ensemble in optical cavities [12, 13]. Recently, an effective and tunable field squeeze operator for a single-mode field or for a two-mode field has been proposed by using an atomic ensemble in an optical cavity [14]. The squeeze operator acts on a cavity with an atomic ensemble but decouples from the atomic degrees of freedom. The squeeze parameter is scaled up with the number of atoms present in the interaction region.

However, to our knowledge, beyond the two-mode case, the multimode squeeze operator [15, 16] has not yet been proposed or realized for atomic systems. Here we propose a mechanism for it. The multimode squeezing is of the particular importance since it is closely correlated to the fully inseparable multipartite states. Such multipartite inseparability is called the genuine multipartite entanglement. This term refers to states, in which none of the parties can be separated from any other party in a mixture of product states. One of important types of genuine multipartite entanglement is Greenberger-Horne-Zeilinger (GHZ) entanglement [17]. In particular, the tripartite CV GHZ state is a three-mode momentum (position) eigenstate with total momentum $p_1+p_2+p_3=0$ (total position $x_1+x_2+x_3=0$) and relative positions $x_k-x_l=0$ (relative momenta $p_k-p_l=0$), $k,l=1,2,3$, $k\neq l$, and exhibits maximum entanglement. Genuine multipartite entanglement enables one to construct a quantum teleportation network [18–20] or to perform controlled dense coding [21, 22]. Loock and Furusawa [23] presented experimental criteria to detect genuine multipartite CV entanglement by using variances of particular combinations of all the quadratures involved. These combinations are measurable with only a few simple homodyne detections. Experimental preparation has been performed by using independent squeezed fields and beam splitters [19–21]. So far experimental research comes to the four-mode case [20].

On the other hand, the atom-field interactions are fundamental mechanisms for creating the multipartite entanglement without use of initially prepared squeezing. For the two-mode case, by using an ensemble of coherently driven two-level atoms one can generate CV entanglement [24–26]. The atom absorbs two photons from the strong driving field and emits two new photons at a pair of Rabi sidebands into the cavity modes [27, 28]. Such a two-photon process is responsible for the nonclassical correlation. In order to obtain multipartite entanglement one turns to multilevel atomic systems [29–32], in which atomic coherent effects are particularly important. Among others is coherent population trapping (CPT) [3, 33], which has been intensively studied for it sets up a basis for various coherence phenomena such

*Author for correspondence. Email: xmhu@phy.ccnu.edu.cn.

as electromagnetically induced transparency and quantum control of photons [34–37], amplification and lasing without inversion [38–43], enhancement of nonlinear optical processes [44–47], and modifications of spontaneous emission [48–52].

The purpose of the present paper is to use the atomic coherent effects to engineer a multimode squeeze operator. We exemplify three- and four-mode cases and derive the squeeze operators, which are decoupled from the atomic degrees of freedom. The squeeze parameters can be large since they are proportional to the number of atoms. According to the relation between the input and output fields, ideal multimode squeezed states and perfect squeezing are achievable. At the same time one can obtain multipartite CV GHZ entangled states. Physically, the atomic coherent effects [3, 33] and parametric interactions [27, 28] combine to be responsible for squeezing and entanglement. In principle, the present scheme is scalable by including more transition channels. The remaining part of the present paper is organized as follows. In Sec. II, we present the model and derive the squeeze operator for the four cavity fields. In Sec. III, we analyze the quantum correlations and show the squeezing and entanglement for three and four fields. The conclusion is given in Sec. IV.

II. SQUEEZE OPERATORS FOR THREE OR FOUR MODES

We consider an ensemble of N-independent atoms that are placed in a four-mode optical cavity, as shown in Fig. 1. The interactions of the atoms with the driving fields and the cavity fields are described in Fig. 2. The atom has three levels, of which one is the ground state $|0\rangle$ and the other two are excited states $|1\rangle$ and $|2\rangle$. As usual, the driving fields are treated classically and the cavity fields are treated quantum mechanically. Two external driving fields of circular frequencies $\omega_{1,2}$ are applied to the dipole-allowed transitions $|0\rangle - |1,2\rangle$ with Rabi frequencies $\Omega_j e^{i\psi_j}$ $(j = 1, 2)$, respectively, where Ω_j are the real amplitudes and ψ_j are the phases. Four sidebands of circular frequencies ν_l are amplified as four cavity fields, which are described by the annihilation and creation operators a_l and $a_l^\dagger$ $(l = 1 - 4)$. In the rotating wave approximation and in an appropriate rotating frame, we derive the master equation for the density operator ρ of the atom-field composite system as [3]

$$\dot{\rho} = -\frac{i}{\hbar}[H, \rho] + \mathcal{L}\rho, \tag{1}$$

with the Hamiltonian $H = H_0 + H_1$, where

$$H_0 = \sum_{j=1}^{2}\sum_{\mu=1}^{N} \hbar[\Delta_j \sigma_{jj}^{\mu} + \frac{\Omega_j}{2}(e^{-i\psi_j}\sigma_{0j}^{\mu} + e^{i\psi_j}\sigma_{j0}^{\mu})], \tag{2}$$

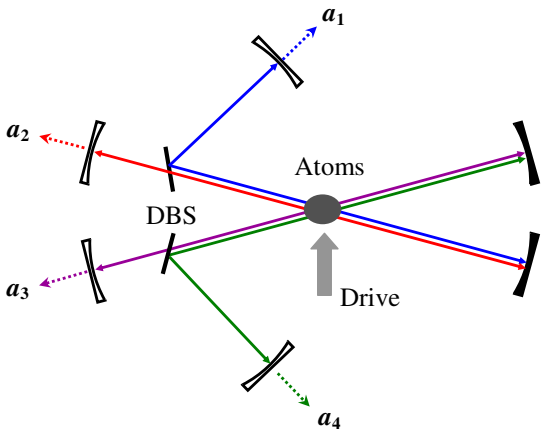

FIG. 1: (Color online) The possible setup for the creation of GHZ entanglement of four cavity fields (denoted by the annihilation operators a_{1-4}).

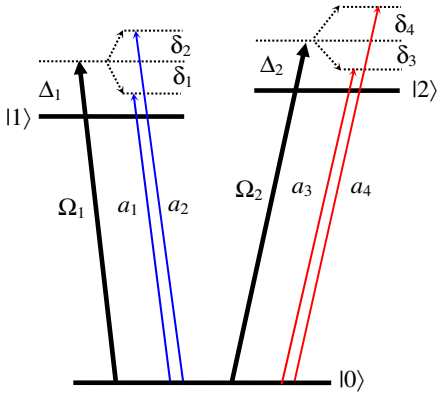

FIG. 2: (Color online) Level scheme for the interactions of two driving fields (denoted by Rabi frequencies $\Omega_{1,2}$) and four cavity fields with an atom in V configuration. Δ's and δ's are the detunings, which are defined in the text.

describes the interaction of the driving fields with the atoms, and

$$H_1 = \sum_{j=1}^{2}\sum_{\mu=1}^{N} \hbar\sigma_{j0}^{\mu}(g_{2j-1}a_{2j-1}e^{-i\delta_{2j-1}t} + g_{2j}a_{2j}e^{-i\delta_{2j}t}) + \text{H.c.}, \tag{3}$$

represents the interaction of the cavity fields with atoms. In the above equations, $\hbar$ is the Planck constant and H.c. is the Hermitian conjugate. For the μth atom, $\sigma_{jk}^{\mu} = |j^{\mu}\rangle\langle k^{\mu}|$ $(j, k = 0, 1, 2)$ are the projection operators for $j = k$ and the spin-flip operator for $j \neq k$. g_l are the strengths for the atom-cavity field couplings. $\Delta_j = \omega_{j0} - \omega_j$ $(j = 1, 2)$ are the frequency detunings between the atoms ω_{l0} and the driving fields. $\delta_1 = \nu_1 - \omega_1$, $\delta_2 =$

$\nu_2-\omega_1$, $\delta_3=\nu_3-\omega_2$, and $\delta_4=\nu_4-\omega_2$ are the frequency detunings between the cavity fields and the driving fields. The decay term in Eq. (1) takes the form $\mathcal{L}\rho=\mathcal{L}_a\rho+\mathcal{L}_c\rho$, where

$$\mathcal{L}_a\rho=\sum_{j=1}^{2}\sum_{\mu=1}^{N}\frac{\gamma_j}{2}\mathcal{D}[\sigma_{0j}^{\mu}]\rho, \tag{4}$$

denotes the atomic relaxation, and

$$\mathcal{L}_c\rho=\sum_{l=1}^{4}\frac{\kappa_l}{2}\mathcal{D}[a_l]\rho, \tag{5}$$

stands for the cavity loss. We have defined the superoperator $\mathcal{D}[Q]\rho\equiv[Q\rho,Q^{\dagger}]+[Q,\rho Q^{\dagger}]$ for the atomic operators σ_{0j}^{μ} and the fields operators a_l. $\gamma_{1,2}$ denote the atomic spontaneous decay rates and $\kappa_{1,2,3,4}$ represent the cavity decay rates.

Here we are interested in the dispersive interaction case, where both the driving fields and the cavity fields are far off resonance with atomic bare-state transitions, and the cavity fields are far off resonance with the dressed transitions by the driving fields. In order to show the establishment of a multimode squeeze operator we derive the time evolution of the four cavity fields through the following four steps.

(i) We introduce two orthogonal coherent superposition states of the two excited states [3]. For the Raman two-photon resonance case $\Delta_1=\Delta_2=\Delta$, these superposition states are defined as

$$\begin{aligned}|\tilde{1}\rangle &= \cos\phi e^{-i\psi_1}|1\rangle+\sin\phi e^{-i\psi_2}|2\rangle,\\ |\tilde{2}\rangle &= -\sin\phi e^{i\psi_2}|1\rangle+\cos\phi e^{i\psi_1}|2\rangle,\end{aligned} \tag{6}$$

where we have defined $\cos\phi=\frac{\Omega_1}{\Omega}$, $\sin\phi=\frac{\Omega_2}{\Omega}$, and the effective Rabi frequency $\Omega=\sqrt{\Omega_1^2+\Omega_2^2}$. The Hamiltonian H_0 is rewritten in terms of the superposition states as

$$H_0=\sum_{\mu=1}^{N}\hbar[\Delta(\sigma_{\tilde{1}\tilde{1}}^{\mu}+\sigma_{\tilde{2}\tilde{2}}^{\mu})+\frac{\Omega}{2}(\sigma_{0\tilde{1}}^{\mu}+\sigma_{\tilde{1}0}^{\mu})]. \tag{7}$$

It is seen Hamiltonian (7) that only the superposition state $|\tilde{1}\rangle$ is coupled to the equivalent field with the effective Rabi frequency Ω, while the coherent superposition state $|\tilde{2}\rangle$ is decoupled from the driving fields. This indicates that the superposition state $|\tilde{2}\rangle$ is not populated due to the destructive interference although there are two bare atomic transitions $|0\rangle\rightarrow|1\rangle$ and $|0\rangle\rightarrow|2\rangle$ to populate the excited states $|1\rangle$ and $|2\rangle$. This is the very counterpart of CPT [3, 33–37]. Here we call the coherent effect the "coherent de-population", and the coherent superposition state $|\tilde{2}\rangle$ the "dark state". The physics common to CPT and de-depopulation is destructive interference between excitation transitions. The essential difference lies between them. All population is in the dark state for CPT case, while no population is in the dark state for the coherent de-population case. Since the superposition state $|\tilde{2}\rangle$ is empty, we can drop it in the following treatment.

(ii) We employ the dressed-atom approach [53]. By diagonalizing the Hamiltonian H_0, we write the dressed states in terms of the bare atomic state $|0\rangle$ and superposition state $|\tilde{1}\rangle$ as

$$\begin{aligned}|+\rangle &= \sin\theta|0\rangle+\cos\theta|\tilde{1}\rangle,\\ |-\rangle &= \cos\theta|0\rangle-\sin\theta|\tilde{1}\rangle,\end{aligned} \tag{8}$$

where $\tan(2\theta)=\frac{\Omega}{\Delta}$, $0<\theta<\frac{\pi}{2}$. The dressed states $|\pm\rangle$ have their eigenvalues $\lambda_{\pm}=\frac{\hbar}{2}(\Delta\pm\bar{\Omega})$, where we have used the generalized Rabi frequency $\bar{\Omega}=\sqrt{\Delta^2+\Omega^2}$. In terms of the dressed atomic states, the Hamiltonian (7) is rewritten as $H_0=\sum_{\mu=1}^{N}(\lambda_+\sigma_{++}^{\mu}+\lambda_-\sigma_{--}^{\mu})$, where $\sigma_{\pm\pm}^{\mu}=|\pm^{\mu}\rangle\langle\pm^{\mu}|$. Then the damping term is written in the form

$$\begin{aligned}\mathcal{L}_a\rho= &\sum_{\mu=1}^{N}\frac{\gamma}{2}\{\cos^4\theta\mathcal{D}[\sigma_{-+}^{\mu}]\rho+\sin^4\theta\mathcal{D}[\sigma_{+-}^{\mu}]\rho\\ &+\gamma\cos^2\theta\sin^2\theta\mathcal{D}[\sigma_{++}^{\mu}-\sigma_{--}^{\mu}]\rho\},\end{aligned} \tag{9}$$

where we have assumed $\gamma_1=\gamma_2=\gamma$ for simplicity. In what follows we are interested in the dispersive interaction, for which the cavity fields are far off resonance with the dressed atomic transitions. In this case, the cavity fields do not change the atomic populations [27, 28]. The equation for the expectation values of the projection operators $\bar{\sigma}_{ll}=\frac{1}{N}\sum_{\mu=1}^{N}\langle\sigma_{ll}^{\mu}\rangle$ $(l=+,-)$ is derived as

$$\frac{d\bar{\sigma}_{++}}{dt}=-\gamma\cos^4\theta\bar{\sigma}_{++}+\gamma\sin^4\theta\bar{\sigma}_{--}, \tag{10}$$

together with the closure relation $\bar{\sigma}_{++}+\bar{\sigma}_{--}=1$. At the steady state we obtain the dressed populations

$$\bar{\sigma}_{++}=\frac{\sin^4\theta}{\cos^4\theta+\sin^4\theta},\quad \bar{\sigma}_{--}=\frac{\cos^4\theta}{\cos^4\theta+\sin^4\theta}. \tag{11}$$

The expectation value for the flip operator of the dressed atoms $\bar{\sigma}_{+-}$ follows the following equation in the absence of the cavity fields

$$\frac{d\bar{\sigma}_{+-}}{dt}=(i\bar{\Omega}+\gamma+2\gamma\cos^2\theta\sin^2\theta)\bar{\sigma}_{+-}. \tag{12}$$

From this equation we obtain the expectation value for the flip operator, which takes the oscillating decay from its initial value $\bar{\sigma}_{+-}^{0}$ as

$$\bar{\sigma}_{+-}=\bar{\sigma}_{+-}^{0}e^{i\bar{\Omega}t-\gamma(1+2\cos^2\theta\sin^2\theta)t}. \tag{13}$$

For the far-off resonance case we will consider, the atomic decay is negligibly small compared with the generalized Rabi frequency, i.e., $\bar{\Omega}\doteq|\Delta|\ggg\gamma$.

(iii) We focus on the case where the driving and cavity fields are far off resonance with the atoms. In order to investigate the interaction of the cavity fields with

the dressed atoms, we make a unitary transformation $\exp(-iH_0t/\hbar)$ and transform into the second interaction picture. The Hamiltonian is written in the form

$$H_1 = \sum_{\mu=1}^{N} \hbar[\cos^2\theta(g_1a_1+g_3a_3) - \sin^2\theta(g_2^*a_2^\dagger+g_4^*a_4^\dagger)]\sigma_{+-}^\mu + \text{H.c.}. \quad (14)$$

We tune the cavity fields such that $\delta_1=\delta_3<0$; $\delta_2=\delta_4>0$; $|\delta_l|\gg|\delta_1+\delta_2|$; $(|\Delta|,|\delta_j|)\gg||\Delta|-|\delta_k||\gg(|g_l\langle a_l\rangle|,\gamma)$. This not only guarantees that the superposition state $|\tilde{2}\rangle$ is decoupled from the cavity fields, but also that the cavity fields are far off resonance with the dressed atomic transitions. For $\Delta\gg\Omega$, we have $\cos\theta=1+O(\chi^2)$, $\sin\theta=\chi+O(\chi^3)$, $\bar{\sigma}_{--}=1+O(\chi^4)$, where $\chi=\frac{\Omega}{\Delta}$. Similarly, for $-\Delta\gg\Omega$, we have $\sin\theta=1+O(\chi^2)$, $\cos\theta=-\chi+O(\chi^3)$, $\bar{\sigma}_{++}=1+O(\chi^4)$. This indicates that for the μth atom we can take the populations $\sigma_{--}^\mu\doteq 1$ and $\sigma_{++}^\mu\doteq 0$ for $\Delta\gg\Omega$, and $\sigma_{++}^\mu\doteq 1$ and $\sigma_{--}^\mu\doteq 0$ for $-\Delta\gg\Omega$. At the same time, the expectation value for the flip operator of the dressed atom shows its time dependence $\sigma_{+-}^\mu=\sigma_{+-}^{0\mu}e^{i\bar{\Omega}t-\gamma t}$. For the far off resonance case, we can derive the effective Hamiltonian as $H_{eff}=-\frac{i}{\hbar}H_1(t)\int H_1(t')dt'$, where the indefinite integral is evaluated at time t without a constant of integration [54]. When $|\delta_l(|\Delta|-|\delta_l|)|\gg|g_l|^2N$ is satisfied the Stark shift of the dressed atoms due to the cavity fields is negligibly small. After discarding the fast oscillating terms, we obtain the effective Hamiltonian

$$H_{eff} = \hbar(\xi_{12}^*a_1a_2+\xi_{32}^*a_3a_2+\xi_{14}^*a_1a_4+\xi_{34}^*a_3a_4) + \text{H.c.}, \quad (15)$$

where the cross coupling coefficients between the cavity fields read

$$\begin{aligned}\xi_{12} &= \frac{g_1^*g_2^*N\Omega_1^2e^{2i\psi_1}}{\Delta^2(|\Delta|-\delta_2+i\gamma)},\\ \xi_{32} &= \frac{g_3^*g_2^*N\Omega_1\Omega_2e^{i(\psi_1+\psi_2)}}{\Delta^2(|\Delta|-\delta_2+i\gamma)},\\ \xi_{14} &= \frac{g_1^*g_4^*N\Omega_1\Omega_2e^{i(\psi_1+\psi_2)}}{\Delta^2(|\Delta|-\delta_2+i\gamma)},\\ \xi_{34} &= \frac{g_3^*g_4^*N\Omega_2^2e^{2i\psi_2}}{\Delta^2(|\Delta|-\delta_2+i\gamma)}. \end{aligned} \quad (16)$$

Hamiltonian (15) indicates the four simultaneous parametric processes: (i) $|0\rangle\xrightarrow{\Omega_1}|1\rangle\xrightarrow{a_1}|0\rangle\xrightarrow{\Omega_1}|1\rangle\xrightarrow{a_2}|0\rangle$, (ii) $|0\rangle\xrightarrow{\Omega_1}|1\rangle\xrightarrow{a_2}|0\rangle\xrightarrow{\Omega_2}|2\rangle\xrightarrow{a_3}|0\rangle$, (iii) $|0\rangle\xrightarrow{\Omega_1}|1\rangle\xrightarrow{a_1}|0\rangle\xrightarrow{\Omega_2}|2\rangle\xrightarrow{a_4}|0\rangle$, (iv) $|0\rangle\xrightarrow{\Omega_2}|2\rangle\xrightarrow{a_3}|0\rangle\xrightarrow{\Omega_2}|2\rangle\xrightarrow{a_4}|0\rangle$. The simultaneous occurrence of these processes is due to the atomic coherent effect stated as in step (i). In Eq. (16), we keep the atomic decay γ although it is negligibly small compared with the detuning difference $|\Delta|-\delta_2$. In the following section, we will show that the atomic decay has a negligible effect on the quantum correlations for the far off resonance case, on which we focus.

(iv) After performing the above three steps and deriving the effective Hamiltonian, we obtain a time evolution, which yields a 4-mode squeeze operator [15, 16]

$$S_4=e^{\varepsilon_{12}^*a_1a_2+\varepsilon_{32}^*a_3a_2+\varepsilon_{14}^*a_1a_4+\varepsilon_{34}^*a_3a_4+\text{H.c.}}, \quad (17)$$

where we have defined the squeezing parameters $\varepsilon_{kl}=i\xi_{kl}^*\tau$ $(k=1,3;l=2,4)$, and τ is the time. For given evolution time τ, the squeeze parameters ε_{kl} can take large values since they are proportional to the number of atoms N. In the absence of any one of four modes (for example, when there is no cavity resonance for a_4), we can obtain a squeeze operator for 3-mode field

$$S_3=e^{\varepsilon_{12}^*a_1a_2+\varepsilon_{32}^*a_3a_2+\text{H.c.}}. \quad (18)$$

Since such a multimode squeeze operator can be established, a multimode field initially in its vacuum state will evolve into a squeezed state.

It is straight to generalize to more modes by including more transitions in the present scheme. We can examine the dependence of the cross coupling strengths on the number n of the transitions involved. When the l-transition is driven by an external coherent field with Rabi frequency Ω_l, the effective Rabi frequency becomes $\Omega=\sqrt{\sum_{l=1}^n\Omega_l^2}$. In order to guarantee the dispersive interactions, we must always take large detuning $|\Delta|\gg\Omega$, whatever positive integer n we are given. Instead, the detuning difference $|\Delta|-\delta_2$ remains unchanged when the cavity fields are properly tuned. In this case, the coupling parameters $\xi_{2j-1,2k}$ between the cavity modes a_{2j-1} and a_{2k} depend on the Rabi frequencies through the relation

$$\xi_{2j-1,2k}\propto\frac{\Omega_j\Omega_k}{\sum_{l=1}^n\Omega_l^2}, \quad (19)$$

where $j\le k$; $j,k=1,2,\cdots,n$. For equal Rabi frequencies we have a simple relation $\xi_{2j-1,2k}\propto\frac{1}{n}$, which indicates that the coupling strengths decrease inversely-proportionally with the number n of the involved transitions.

III. GHZ ENTANGLEMENT FOR THREE OR FOUR PARTIES

In the following section, we exemplify three and four modes and show that ideal squeezed states and perfect squeezing could be approached at the output port. At the same time, we show that tripartite and quadripartite GHZ entangled states can be obtainable. In order to investigate the multimode correlations, we first define the quadrature operators for each mode as

$$x_l=a_l+a_l^\dagger, \qquad p_l=-i(a_l-a_l^\dagger), \quad (20)$$

such that $[x_l\ , p_l] = 2i$, $l = 1 - 4$. Then the quadrature operators for $n \geq 3$ modes can be defined as

$$X_n = \frac{1}{\sqrt{n}} \sum_{l=1}^{n} x_l, \quad Y_n = \frac{1}{\sqrt{n}} \sum_{l=1}^{n} p_l. \tag{21}$$

If the variances for certain quadratures have fluctuations below the standard quantum limit one has n-mode squeezing. We define the variances $V_{X_n} = \langle (\delta X_n)^2 \rangle$ and $V_{Y_n} = \langle (\delta Y_n)^2 \rangle$ for operators X_n and Y_n, respectively. Squeezing occurs when $V_{X_n} < 1$ or $V_{Y_n} < 1$.

We learn that for three cavity fields $a_{1,2,3}$, two conditions are sufficient to verify the CV GHZ entangled state [23]. These two conditions are

$$\begin{aligned} U_{12} &= V(x_1 + x_2) + V(p_1 - p_2 + h_3 p_3) < 4, \\ U_{23} &= V(x_2 + x_3) + V(p_2 - p_3 + h_1 p_1) < 4, \end{aligned} \tag{22}$$

where h_l ($l = 1, 3$) are arbitrary real parameters that are used to optimize the correlations. The optimization parameters are obtained by minimizing the variances as

$$h_1 = \frac{V_{31} - V_{21}}{V_{11}}, \quad h_3 = \frac{V_{23} - V_{13}}{V_{33}}, \tag{23}$$

where $V_{kl} = \frac{1}{2}(\langle \delta p_k \delta p_l \rangle + \langle \delta p_l \delta p_k \rangle)$. For four cavity fields, there are three inequalities that are sufficient for the GHZ entanglement [23]

$$\begin{aligned} U_{34} &= V(x_3 + x_4) + V(p_3 - p_4 + h_1 p_1 + h_2 p_2) < 4, \\ U_{14} &= V(x_1 + x_4) + V(p_1 - p_4 + h_2 p_2 + h_3 p_3) < 4, \\ U_{23} &= V(x_2 + x_3) + V(p_2 - p_3 + h_1 p_1 + h_4 p_4) < 4, \end{aligned} \tag{24}$$

where the optimization parameters h_l ($l = 1 - 4$) are derived as

$$\begin{aligned} h_1 &= \frac{V_{44}(V_{12} - V_{13}) - V_{14}(V_{24} - V_{34})}{V_{14}^2 - V_{11} V_{44}}, \\ h_2 &= \frac{V_{33}(V_{12} - V_{24}) - V_{23}(V_{13} - V_{34})}{V_{23}^2 - V_{22} V_{33}}, \\ h_3 &= \frac{V_{22}(V_{13} - V_{34}) - V_{23}(V_{12} - V_{24})}{V_{23}^2 - V_{22} V_{33}}, \\ h_4 &= \frac{V_{11}(V_{24} - V_{34}) - V_{14}(V_{12} - V_{13})}{V_{14}^2 - V_{11} V_{44}}. \end{aligned} \tag{25}$$

For the present system, since the cavity fields are decoupled from the atomic degrees of freedom, we have the master equation for the reduced density operator ρ_c of the cavity fields

$$\dot{\rho}_c = -\frac{i}{\hbar}[H_{eff}, \rho_c] + \mathcal{L}_c \rho_c, \tag{26}$$

where the effective Hamiltonian and the cavity damping are given in Eq. (15) and Eq. (5), respectively. By means of the generalized P representation of Drummond and Gardiner [55], and from the master equation (26) we can derive the set of Langevin equations. To do this, we choose a definite operator order: $a_1^\dagger, a_2^\dagger, a_3^\dagger, a_4^\dagger, a_4, a_3, a_2, a_1$, and use the correspondences between the c–numbers and the operators: $\alpha_l \leftrightarrow a_l, \alpha_l^* \leftrightarrow a_l^\dagger$ ($l = 1 - 4$). For the sake of simplicity we assume $-i\xi_{kl}$ ($k = 1, 3; l = 2, 4$) to be positive, which is guaranteed by manipulating the phase factors. Then we substitute ξ_{kl} for $-i\xi_{kl}$ and match the standard notation for the two-mode case [56]. The set of Langevin equations are derived as follows

$$\begin{aligned} \dot{\alpha}_1 &= \alpha_1^{in} - \kappa_1' \alpha_1 + \xi_{12} \alpha_2^* + \xi_{14} \alpha_4^* + F_{\alpha_1}(t), \\ \dot{\alpha}_2 &= \alpha_2^{in} - \kappa_2' \alpha_2 + \xi_{12} \alpha_1^* + \xi_{32} \alpha_3^* + F_{\alpha_2}(t), \\ \dot{\alpha}_3 &= \alpha_3^{in} - \kappa_3' \alpha_3 + \xi_{32} \alpha_2^* + \xi_{34} \alpha_4^* + F_{\alpha_3}(t), \\ \dot{\alpha}_4 &= \alpha_4^{in} - \kappa_4' \alpha_4 + \xi_{14} \alpha_1^* + \xi_{34} \alpha_3^* + F_{\alpha_4}(t), \end{aligned} \tag{27}$$

together with those for α_l^* ($l = 1 - 4$). In the above equations, α_l^{in} are the average amplitudes for the input fields, and $\kappa_l' = \frac{\kappa_l}{2}$. $F_{\alpha_l}(t)$ are the Langevin fluctuation forces and are assumed to be δ correlated, satisfying $\langle F_{\alpha_k}(t) F_{\alpha_l}(t') \rangle = D_{\alpha_k \alpha_l} \delta(t - t')$. The nonzero diffusion coefficients are $D_{\alpha_1 \alpha_2} = -\xi_{12}$, $D_{\alpha_2 \alpha_3} = -\xi_{32}$, $D_{\alpha_1 \alpha_4} = -\xi_{14}$, and $D_{\alpha_3 \alpha_4} = -\xi_{34}$, $D_{\alpha_l \alpha_k} = D_{\alpha_k \alpha_l}$, and $D_{\alpha_k^* \alpha_l^*} = D_{\alpha_k \alpha_l}$. By writing $\alpha_l = \langle \alpha_l \rangle + \delta \alpha_l$ and describing to first order the fluctuations in the field variables, we obtain the linearized Langevin equations, which are given in a compact form

$$\frac{d}{dt} \delta X(t) = -B \delta X(t) + F(t), \tag{28}$$

where $\delta X(t) = (\delta \alpha_1, \delta \alpha_2, \delta \alpha_3, \delta \alpha_4, \delta \alpha_1^*, \delta \alpha_2^*, \delta \alpha_3^*, \delta \alpha_4^*)^T$, $F(t) = (F_{\alpha_1}, F_{\alpha_2}, F_{\alpha_3}, F_{\alpha_4}, F_{\alpha_1^*}, F_{\alpha_2^*}, F_{\alpha_3^*}, F_{\alpha_4^*})^T$, where the drift matrix G can easily be obtained from Eq. (27). The correlation matrix for the noise term $\langle F(t) F^T(t') \rangle = D \delta(t - t')$ is easily obtained from the above diffusion coefficients. The system reaches its steady state and is stable when all of the eigenvalues of G have positive real parts. The linearized Langevin equations (28) can be rewritten in the spectral form. Defining the Fourier transformation $\delta R(\omega) = \frac{1}{\sqrt{2\pi}} \int dt e^{-i\omega t} \delta R(t)$, we write the correlation spectrum as $\langle \delta R(\omega) \delta R^T(\omega') \rangle = S(\omega) \delta(\omega + \omega')$, where $S(\omega)$ is derived as

$$S(\omega) = (B - i\omega I)^{-1} D (B^T + i\omega I)^{-1}, \tag{29}$$

where I is a unit matrix.

We present the measurable spectral quantities for the optical fields outside the cavity. By $V_{X_n}(\omega)$, $V_{Y_n}(\omega)$, and $U_{kl}(\omega)$ we denote the output spectra for the correlations $V(X_n)$, $V(Y_n)$, and U_{kl}, respectively. We use the input-output relations [2, 56] $a_l^{in} + a_l^{out} = \sqrt{\kappa_l} a_l$ and assume the coherent inputs. Defining the correlation spectra $\langle \delta O_1 \delta O_2 \rangle(\omega) \delta(\omega + \omega') = \langle \delta O_1(\omega) \delta O_2(\omega') \rangle$ for arbitrary two operators O_1 and O_2, we relate the output spectra to the intracavity spectra through the relations

$$\begin{aligned} \langle \delta x_k^o \delta x_l^o \rangle(\omega) &= (-1)^{k-l} \langle \delta p_k^o \delta p_l^o \rangle(\omega) \\ &= \delta_{kl} + \sqrt{\kappa_k \kappa_l} \langle \delta x_k \delta x_l \rangle(\omega), \end{aligned} \tag{30}$$

where we have used Kronecker delta function $\delta_{kl} = 1$ for $k = l$, and otherwise $\delta_{kl} = 0$.

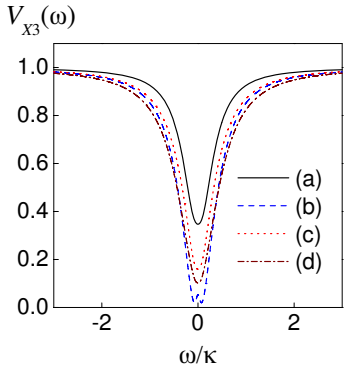

FIG. 3: (Color online) The three-mode correlation spectrum $V_{X_3}(\omega)$ for various parameters as in the text.

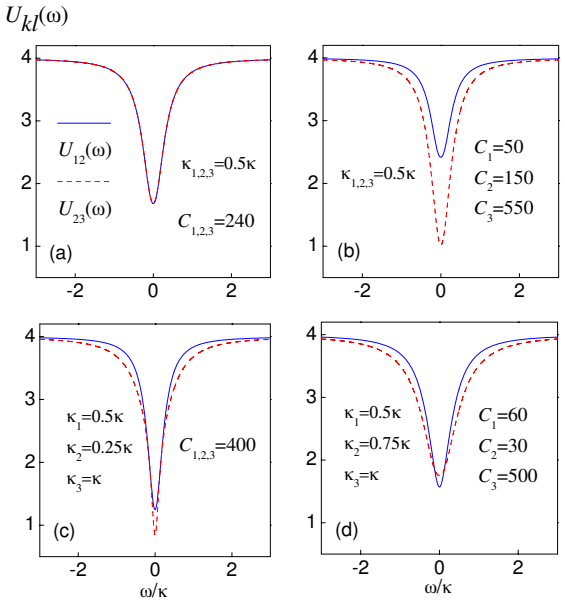

FIG. 4: (Color online) The correlation spectra $U_{12}(\omega)$ (solid) and $U_{23}(\omega)$ (dashed) for various cases of different parameters.

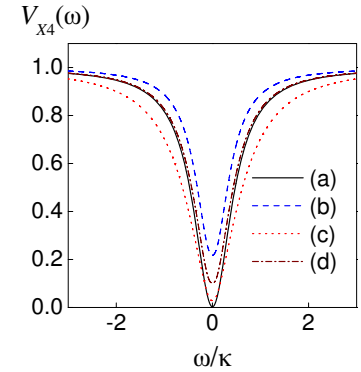

FIG. 5: (Color online) The four-mode correlation spectrum $V_{X_4}(\omega)$ for various parameters as in the text.

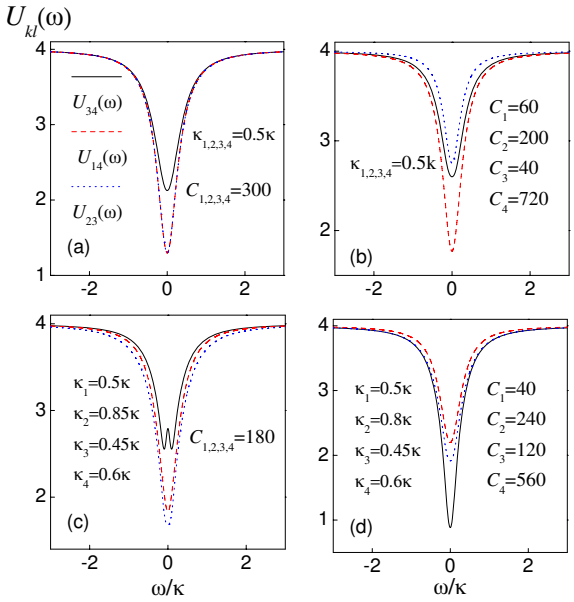

FIG. 6: (Color online) The correlation spectra $U_{34}(\omega)$ (solid), $U_{14}(\omega)$ (dashed), and $U_{23}(\omega)$ (dotted) for various cases of different parameters.

In what follows we present the numerical results. The cooperativity parameters are defined as $C_l = \frac{g_l^2 N}{\kappa_l^2}$, which are associated with the different modes a_l $(l = 1-4)$. As the first step we assume that γ is negligibly small compared with the detuning $|\Delta| - \delta_2$. We rescale the decay rates, detunings, Rabi frequencies, and Fourier frequency in units of a rate parameter κ MHz. The parameters are chosen as $\Omega_1 = \Omega_2$ and $\frac{\Omega^2}{\Delta^2}(|\Delta| - \delta_2)^{-1} = 2 \times 10^{-3}\kappa^{-1}$. We first give the numerical results for the three-mode case, which are obtained simply by removing any one of four modes. For definiteness we remove the a_4 mode. Plotted in Fig. 3 is the three-mode correlation spectrum $V_{X_3}(\omega)$ for various values of cavity loss rates and cooperativity parameters: (a) $\kappa_{1,2,3} = 0.5\kappa, C_{1,2,3} = 250$; (b) $\kappa_{1,2,3} = 0.5\kappa, C_1 = 120, C_2 = 400, C_3 = 1200$; (c) $\kappa_1 = 0.5\kappa, \kappa_2 = 0.4\kappa, \kappa_3 = \kappa, C_{1,2,3} = 330$; and (d) $\kappa_1 = 0.5\kappa, \kappa_2 = 0.8\kappa, \kappa_3 = 0.4\kappa, C_1 = 40, C_2 = 800, C_3 = 400$. It is seen that for various choices of parameters, the fluctuation spectrum drops below the standard quantum limit 1. This means that the three-mode quadrature X_3 has the reduced fluctuations. For a certain case (e.g., (b)), the fluctuations are reduced to the zero level, which shows the ideal squeezed states and perfect squeezing. In Fig. 4 we plot the two correlation spectra $U_{12}(\omega)$ and $U_{23}(\omega)$ for (a) $\kappa_{1,2,3} = 0.5\kappa$, $C_{1,2,3} = 240$; (b) $\kappa_{1,2,3} = 0.5\kappa$, $C_1 = 50, C_2 = 150, C_3 = 550$; (c) $\kappa_1 = 0.5\kappa, \kappa_2 = 0.25\kappa, \kappa_3 = \kappa, C_{1,2,3} = 400$; and (d) $\kappa_1 = 0.5\kappa, \kappa_2 = 0.75\kappa, \kappa_3 = \kappa, C_1 = 60, C_2 = 500, C_3 = 30$. For the identical cavity loss rates and the identical cooperativity parameters (Fig. 4(a)), the curves for the correlation spectra $U_{12}(\omega)$ and $U_{23}(\omega)$ display the same dip. In terms of correlation spectra, the criteria (22) in the spectral form are well satisfied, which shows that

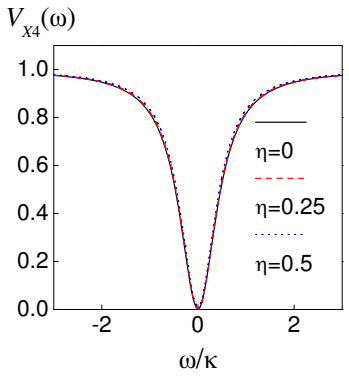

FIG. 7: (Color online) The four-mode correlation spectrum $V_{X_4}(\omega)$ for $\eta = 0$ (solid), $\eta = 0.25$ (dashed) and $\eta = 0.5$ (dotted). The other parameters are taken from Fig. 5(a).

GHZ entanglement occurs for three cavity fields $a_{1,2,3}$. The criteria are also well satisfied for various cases of different parameters (Fig. 4(b-d)).

Similarly, we show in Fig. 5 and Fig. 6 the existence of squeezing and GHZ entanglement for four cavity fields. Plotted in Fig. 5 is the correlation spectrum $V_{X_4}(\omega)$ for (a) $\kappa_{1,2,3,4} = 0.5\kappa, C_{1,2,3,4} = 450$; (b) $\kappa_{1,2,3,4} = 0.5\kappa$, $C_1 = 120, C_2 = 60, C_3 = 480, C_4 = 600$; (c) $\kappa_1 = 0.5\kappa, \kappa_2 = 0.6\kappa, \kappa_3 = \kappa, \kappa_4 = 0.75\kappa$, $C_{1,2,3,4} = 300$; and (d) $\kappa_1 = 0.5\kappa, \kappa_2 = 0.9\kappa, \kappa_3 = 0.6\kappa, \kappa_4 = 0.45\kappa$, $C_1 = 420, C_2 = 90, C_3 = 180, C_4 = 720$. We see that $V_{X_4}(\omega)$ is reduced below the standard quantum limit 1, which indicates the appearance of four-mode squeezing. For the symmetrical case of parameters as in Fig. 5(a), the dip drops to zero, which corresponds to the perfect squeezing and ideal squeezed states. Shown in Fig. 6 are the correlation spectra $U_{34}(\omega)$ (solid), $U_{14}(\omega)$ (dashed), and $U_{23}(\omega)$ (dotted) for (a) $\kappa_{1,2,3,4} = 0.5\kappa, C_{1,2,3,4} = 200$; (b) $\kappa_{1,2,3,4} = 0.5\kappa$, $C_1 = 60, C_2 = 200, C_3 = 40, C_4 = 720$; (c) $\kappa_1 = 0.5\kappa, \kappa_2 = 0.85\kappa, \kappa_3 = 0.45\kappa, \kappa_4 = 0.6\kappa, C_{1,2,3,4} = 180$; and (d) $\kappa_1 = 0.5\kappa, \kappa_2 = 0.8\kappa, \kappa_3 = 0.45\kappa, \kappa_4 = 0.6\kappa, C_1 = 40, C_2 = 240, C_3 = 120, C_4 = 560$. It is clear that for a wide range of parameters the criteria (24) in the spectral form are met, which indicates the existence of GHZ entangled state for four cavity fields.

After performing the numerical results we are in a position to analyze the physical mechanism. We recall that coherently driven two-level atoms can be used as a reservoir to generate two-mode CV entanglement[25, 26]. The responsible mechanism is based on the quantum correlations of a pair of sideband photons [27, 28]. The upper and lower sideband photons are generated simultaneously when the atoms absorb two photons from the strong driving field. In the large detuning limit, the initial atomic population is not significantly changed, and a parametric process based on the two-photon transition is created. When only the modes $a_{1,2}$ are present, Eq. (17) reduces to a two-mode squeeze operator. Such a mechanism holds for the case where there are only the modes $a_{3,4}$. When both channels are involved for a_{1-4} modes, we have quantum interference between these two pathways [3, 33–37]. Due to the atomic coherent effects, the odd modes $a_{1,3}$ and the even modes $a_{2,4}$ are in the simultaneous parametric interactions, which determines the four-mode squeeze operator. By including more transitions, we can achieve the squeeze operators for more modes.

So far we have neglected the atomic spontaneous decay. Now we turn to discussing the effects of the atomic decay on the quantum correlations by exemplifying the four-mode case. For the sake of convenience we define the ratio $\eta = \frac{\gamma}{|\Delta|-\delta_2}$, where $|\Delta| - \delta_2$ is the frequency detuning between the dressed atomic resonance and the cavity mode. Fig. 7 gives the four-mode correlation spectrum V_{X_4} for $\eta = 0$ (solid), $\eta = 0.25$ (dashed) and $\eta = 0.5$ (dotted). The other parameters are the same as for the curve (a) in Fig. 5. We see that the correlation spectrum is almost kept unchanged although the decay rate changes so much. Plotted in Fig. 8 are the correlation spectra (i) $U_{34}(\omega)$, (ii) $U_{14}(\omega)$, and (iii) $U_{23}(\omega)$ for $\eta = 0$ (solid), $\eta = 0.25$ (dashed), and $\eta = 0.5$ (dotted). The other parameters are the same as in (b) of Fig. 6. It is clear that the correlation spectra are not significantly influenced. Physically, all fields are far off resonance with atomic transitions, including the dressed transitions. It means that the spectra of the cavity fields locate beyond the spontaneous emission spectrum of the atoms. This is the very advantage of using dispersive interactions as physical mechanisms that generate nonclassical light. The essential difference of the present scheme from the existing ones is the simultaneous dispersive interactions through two or more channels, between which quantum interference is created. It is the quantum interference that plays a crucial role in creating the nonclassical correlations between multiple modes.

A great number of atomic structures can be used as candidates for the present system. For example, for four modes, the atom ^{87}Rb is a candidate, in which we use $|0\rangle = |5S_{1/2}, F = 2\rangle$, $|1\rangle = |5P_{1/2}, F = 3\rangle$ and $|2\rangle = |5P_{3/2}, F = 3\rangle$. The two transitions in the V configuration are well separated from each other by the D_1 line (794.8 nm) and the D_2 line (780.0 nm). In order to avoid the Doppler effect one can use an ensemble of cold atoms, which are prepared a magneto optical trap [12, 13, 57–59]. A rough estimate of the coupling strengths can be made by considering a particular case, $g_l = g$, $\kappa_l = \tilde{\kappa}$ $(l = 1 - 4)$, and $\Omega_j = \tilde{\Omega}$ $(j = 1, 2)$. In this case we have equal cross coupling coefficients, $|\xi_{2j-1,2k}| = \xi$ $(j, k = 1, 2)$. For the dispersive interaction we can take parameters $|\Delta| - \delta_2 \sim 4\gamma$, $|\Delta| \sim 25\gamma$, $\tilde{\Omega} \sim 5\gamma$, we have $\frac{\xi}{\tilde{\kappa}} = 10^{-2} C \frac{\tilde{\kappa}}{\gamma}$, where $C = \frac{g^2 N}{\tilde{\kappa}^2}$ is the cooperativity parameter. When the parameter $C\frac{\tilde{\kappa}}{\gamma}$ is in the order of $\sim 10^2$, the cross coupling strength is in the order of the cavity loss rate, $\xi \sim \tilde{\kappa}$. A comparison can be made with the realistic cases with atomic ensembles [12–14, 60–65]. We use the atomic ^{87}Rb D_2 transition with decay rate $\gamma \sim 2\pi \times 5.4$ MHz. For the cavity parameters we choose the waist $w \sim 35$ μm and homogeneous laser

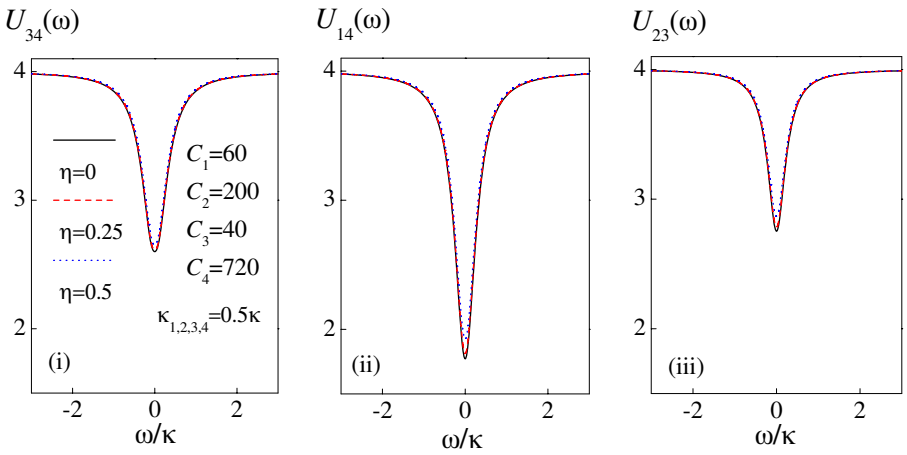

FIG. 8: (Color online) The correlation spectra (i) $U_{34}(\omega)$, (ii) $U_{14}(\omega)$, and (iii) $U_{23}(\omega)$ for $\eta = 0$ (solid), $\eta = 0.25$ (dashed) and $\eta = 0.5$ (dotted). The other parameters are taken from (b) of Fig. 6.

beams of width $d \sim 50$ μm, both of which correspond to an interaction volume of $\sim 10^{-7}$ cm^3. The cavity loss rate takes a value of $\tilde{\kappa} \sim 2\pi \times 2.5$ MHz. For a low density of $\sim 10^{12}/\text{cm}^3$, which is small enough to prevent coherence losses due to collisions, we have $N \sim 10^4$. For the above parameters, the coupling constant is required such that $g \sim 2\pi \times 37$ kHz, which is quite loose condition for the coupling strength. In comparison, a realistic coupling constant takes a value of $g \sim 2\pi \times 100$ kHz. This shows that the present scheme is experimentally accessible within the current technology.

IV. CONCLUSION

In conclusion, by exemplifying four cavity fields we have shown that multimode squeeze operators are obtainable by using atomic coherent effects in a three-level V system. Due to the atomic coherent effects, multiple parametric processes occur simultaneously. The squeeze parameters are large since they are proportional to the number of the involved atoms. This squeeze operator creates multimode squeezed states and multipartite CV GHZ entangled states. The numerical results for the correlation spectra at the output are given for the cases of three and four fields.

Acknowledgements

This work is supported by the National Natural Science Foundation of China (Grants No. 11074086 and 61178021), National Basic Research Program of China (Grant No. 2012CB921604), and Natural Science Foundation of Hubei Province (Grant No. 2010CDA075).

[1] C. M. Caves, K. S. Thorne, R. W. P. Drever,V. D. Sandberg and Zimmermann, Rev. Mod. Phys. **52**, 341 (1980).
[2] D. F. Walls and G. J. Milburn, *Quantum Optics* (Springer-Verlag, Berlin, 1994).
[3] M. O. Scully and M. S. Zubairy, *Quantum Optics* (Cambridge University Press, Cambridge, 1997).
[4] A. Einstein, B. Podolsky and N. Rosen, Phys. Rev. **47**, 777 (1935); M. D. Reid, Phys. Rev. A **40**, 913 (1989).
[5] L. M. Duan, G. Giedke, J. I. Cirac, and P. Zoller, Phys. Rev. Lett. **84**, 2722 (2000).
[6] C. H. Bennett, G. Brassard, C. Crpeau, R. Jozsa, A. Peres, and W. K. Wootters, Phys. Rev. Lett. **70**, 1895 (1993).
[7] L. Vaidman, Phys. Rev. A **49**, 1473 (1994).
[8] S. L. Braunstein and P. van Loock, Rev. Mod. Phys. **77**, 513 (2005).
[9] P. Zoller, T. Beth, D. Binosi, R. Blatt, H. Briegel *et al.*, Eur. Phys. J. D **36**, 203 (2005).
[10] A. Furusawa and N. Takei, Phys. Rep. **443**, 97 (2007).
[11] S. L. Braunstein and H. J. Kimble, Phys. Rev. Lett. **80**, 869 (1998).
[12] V. Josse, A. Dantan, L. Vernac, A. Bramati, M. Pinard and E. Giacobino, Phys. Rev. Lett. **91**, 103601 (2003).
[13] V. Josse, A. Dantan, A. Bramati, M. Pinard and E. Giacobino, Phys. Rev. Lett. **92**, 123601 (2004).
[14] R. Guzmán, J. C. Retamal, E. Solano and N. Zagury, Phys. Rev. Lett. **96**, 010502 (2006).
[15] X. Ma and W. Rhodes, Phys. Rev. A **41**, 4625 (1990).
[16] C. F. Lo and R. Sollie, Phys. Rev. A **47**, 733 (1993).
[17] D. M. Greenberger, M. A. Horne, A. Shimony and A. Zeilinger, Am. J. Phys. **58**, 1131 (1990).
[18] P. van Loock and S. L. Braunstein, Phys. Rev. Lett. **87**, 247901 (2001).
[19] T. Aoki, N. Takei, H. Yonezawa, K. Wakui, T. Hiraoka and A. Furusawa, Phys. Rev. Lett. **91**, 080404 (2003).
[20] X. L. Su, A. H. Tan, X. J. Jia, J. Zhang, C. D. Xie, and K. C. Peng, Phys. Rev. Lett. **98**, 070502 (2007).
[21] J. T. Jing, J. Zhang, Y. Yan, F. G. Zhao, C. D. Xie, and

K. C. Peng, Phys. Rev. Lett. **90**, 167903 (2003).
[22] J. Zhang, C. Xie, and K. Peng, Phys. Rev. A **66**, 032318 (2002).
[23] P. van Loock and A. Furusawa, Phys. Rev. A **67**, 052315 (2003).
[24] H. Xiong, M. O. Scully and M. S. Zubairy, Phys. Rev. Lett. **94**, 023601 (2005).
[25] S. Pielawa, G. Morigi, D. Vitali and L. Davidovich, Phys. Rev. Lett. **98**, 240401 (2007).
[26] M. Ikram, G. X. Li and M. S. Zubairy, Phys. Rev. A **76**, 042317 (2007).
[27] P. Meystre and M. Sargent, *Elements of Quantum Optics* 2nd edn (Springer, Berlin, 1990).
[28] R. W. Boyd, *Nonlinear Optics* (Academic Press, Boston, 1992).
[29] Y. Wu and L. Deng, Opt. Lett. **29**, 1144; 2064 (2004).
[30] X. X. Li and X. M. Hu, Phys. Rev. A **80**, 023815 (2009); X. Zhang and X. M. Hu, Phys. Rev. A **81**, 013811 (2010).
[31] H. T. Tan and G. X. Li, Phys. Rev. A **82**, 032322 (2010).
[32] X. Y. Lü and J. Wu, Phys. Rev. A **82**, 012323 (2010).
[33] E. Arimondo, in *Progress in Optics*, edited by E. Wolf, Vol. 35 (Elsevier Science, Amsterdam, 1996), p. 257.
[34] S. E. Harris, Phys. Today **50**, (7) 36 (1997).
[35] J. P. Marangos, J. Mod. Opt. **45**, 471 (1998).
[36] M. D. Lukin, Rev. Mod. Phys. **75**, 457 (2003).
[37] M. Fleischhauer, A. Imamoglu, and J. P. Marangos, Rev. Mod. Phys. **77**, 633 (2005).
[38] M. O. Scully, Phys. Rep. **219**, 191 (1992).
[39] O. Kocharovskaya, Phys. Rep. **219**, 175 (1992).
[40] P. Mandel, Contemp. Phys. **34**, 235 (1993).
[41] A. S. Zibrov, M. D. Lukin, D. E. Nikonov, L. Hollberg, M. O. Scully, V. L. Velichansky and H. G. Robinson, Phys. Rev. Lett. **75**, 1499 (1995).
[42] G. G. Padmabandu, G. R. Welch, I. N. Shubin, E. S. Fry, D. E. Nikonov, M. D. Lukin and M. O. Scully, Phys. Rev. Lett. **76**, 2053 (1996).
[43] J. Mompart and R. Corbalan, J. Opt. B: Quantum Semiclassical Opt. **2**, R7 (2000).
[44] H. Wang, D. Goorskey and M. Xiao, Phys. Rev. Lett. **87**, 073601 (2001).
[45] H. Schmidt and A. Imamoglu, Opt. Lett. **21**, 1936 (1996).
[46] J. Sun, Z. C. Zuo, X. Mi, Z. H. Yu, Q. Jiang, Y. B. Wang, L. A. Wu and P. M. Fu, Phys. Rev. A **70**, 053820 (2004).
[47] X. M. Hu, G. L. Cheng, J. H. Zou, X. Li and D. Du, Phys. Rev. A **72**, 023803 (2005).
[48] S. Y. Zhu and M. O. Scully, Phys. Rev. Lett. **76**, 388 (1996).
[49] P. Zhou and S. Swain, Phys. Rev. Lett. **77**, 3995 (1996).
[50] E. Paspalakis and P. L. Knight, Phys. Rev. Lett. **81**, 293 (1998).
[51] C. H. Keitel, Phys. Rev. Lett. **83**, 1307 (1999).
[52] X. M. Hu, W. X. Shi, Q. Xu, H. J. Guo, J. Y. Li and X. X. Li, Phys. Lett. A **352**, 543 (2006).
[53] C. Cohen-Tannoudji, J. Dupont-Roc and G. Grynberg, *Atom-Photon Interactions* (Wiley, New York, 1992).
[54] D. F. V. James, Fortschr. Phys. **48**, 823 (2000).
[55] P. D. Drummond and C. W. Gardiner, J. Phys. A **13**, 2353 (1980); P. D. Drummond and D. F. Walls, Phys. Rev. A **23**, 2563 (1981).
[56] C. W. Gardiner and P. Zoller, *Quantum Noise*, 2nd ed. (Springer-Verlag, Berlin, 2000).
[57] H. Kang, G. Hernandez, and Y. Zhu, Phys. Rev. Lett. **91**, 093601 (2003) **93**, 073601 (2004).
[58] Y. F. Chen, C. Y. Wang, S. H. Wang, and I. A. Yu, Phys. Rev. Lett. **96**, 043603 (2006).
[59] J. Zhang, J. Xu, G. Hernandez, X. M. Hu, and Y. Zhu, Phys. Rev. A **75**, 043810 (2007).
[60] A. Kuzmich, Klaus Mølmer, and E. S. Polzik, Phys. Rev. Lett. **79**, 4782 (1997).
[61] A. S. Sørensen and K. Mølmer, Phys. Rev. A **66**, 022314 (2002).
[62] B. Julsgaard, J. Sherson, J. I. Cirac, J. Fiurášek, and E. S. Polzik, Nature (London) **432**, 482 (2004).
[63] A. Dantan, A. Bramati, and M. Pinard, Phys. Rev. A **71**, 043801 (2005).
[64] J. K. Thompson, J. Simon, H. Loh and V. Vuletić, Science **313**, 74 (2006).
[65] K. Hammerer, A. S. Sørensen, and E. S. Polzik, Rev. Mod. Phys. **82**, 1041 (2010).